

Infrared spectroscopy of SWIFT J0850.8-4219: Identification of the second red supergiant X-ray binary in the Milky Way

Kishalay De,^{1,2}★ Fiona A. Daly,¹ and Roberto Soria^{3,4,5}

¹MIT-Kavli Institute for Astrophysics and Space Research, 77 Massachusetts Ave., Cambridge, MA 02139, USA

²NASA Einstein Fellow

³College of Astronomy and Space Sciences, University of the Chinese Academy of Sciences, Beijing 100049, China

⁴INAF – Osservatorio Astrofisico di Torino, Strada Osservatorio 20, I-10025 Pino Torinese, Italy

⁵Sydney Institute for Astronomy, School of Physics A28, The University of Sydney, Sydney, NSW 2006, Australia

Accepted XXX. Received YYY; in original form ZZZ

ABSTRACT

High mass X-ray binaries hosting red supergiant (RSG) donors are a rare but crucial phase in massive stellar evolution, with only one source previously known in the Milky Way. In this letter, we present the identification of the second Galactic RSG X-ray binary SWIFT J0850.8-4219. We identify the source 2MASS 08504008-4211514 as the likely infrared counterpart with a chance coincidence probability $\approx 5 \times 10^{-6}$. We present a $1.0 - 2.5 \mu\text{m}$ spectrum of the counterpart, exhibiting features characteristic of late-type stars and an exceptionally strong He I emission line, corroborating the identification. Based on i) the strength of the $^{12}\text{CO}(2,0)$ band, ii) strong CN bandheads and absent TiO bandheads at $\approx 1.1 \mu\text{m}$ and iii) equivalent width of the Mg I $1.71 \mu\text{m}$ line, we classify the counterpart to be a K3–K5 type RSG with an effective temperature of $3820 \pm 100 \text{ K}$, located at a distance of $\approx 12 \text{ kpc}$. We estimate the source X-ray luminosity to be $(4 \pm 1) \times 10^{35} \text{ erg s}^{-1}$, with a hard photon index ($\Gamma < 1$), arguing against a white dwarf accretor but consistent with a magnetized neutron star in the propeller phase. Our results highlight the potential of systematic NIR spectroscopy of Galactic hard X-ray sources in completing our census of the local X-ray binary population.

Key words: X-rays: binaries – accretion – stars: supergiants – stars: evolution

1 INTRODUCTION

Symbiotic X-ray binaries (SyXBs) are a rare class of X-ray binaries consisting of a neutron star (NS) or black hole (BH) accreting from the wind of a very late-type giant companion (Davidsen et al. 1977). There are only 14 known SyXBs in the Milky Way (Yungelson et al. 2019; De et al. 2022) compared to the hundreds of other known classes of X-ray binaries (Liu et al. 2007). Given their short-lived lifetimes as well as rare formation pathways (e.g. Kuranov et al. 2015; Hinkle et al. 2006), population synthesis models predict that there are only ≈ 50 active SyXBs in the Galaxy. Nearly all known SyXBs consist of a low mass giant donor; the SyXB Scutum X-1 was proposed to be the first known SyXB with a red supergiant (RSG) companion (Kaplan et al. 2007), although the source has been recently confirmed to host the first confirmed Mira variable donor in a XRB (De et al. 2022). Hinkle et al. (2020) recently showed that the late-type donor in the SyXB 4U 1954+31 was long mis-classified as a low mass giant; instead the infrared luminosity and spectra are consistent with a RSG donor.

4U 1954+31 remains as the only known RSG X-ray binary in the Milky Way. With a $\approx 7 - 15 M_{\odot}$ donor, this source is the only high mass X-ray binary (HMXB) with a late-type donor, compared to the > 100 known HMXBs with blue supergiant donors (Chaty 2018), reflecting the extremely short-lived lifetime of the RSG phase. In

addition, the survival of the binary up to the SyXB phase requires fine-tuned conditions to ensure that the supernova (SN) that created the compact object had sufficiently low ejecta mass and kick velocity to prevent the disruption of the binary. Indeed, Hinkle et al. (2020) invoked a low mass core-collapse SN from an ultra-stripped progenitor (Tauris et al. 2015; De et al. 2018) to explain the existence of the RSG in 4U 1954+31. Following the lifetime of the RSG, the final fate of such systems involve the likely creation of a double NS binary, which may merge producing detectable gravitational waves if the orbital period of the resulting double NS binary is short enough (Tauris & van den Heuvel 2006; Tauris et al. 2017).

As such, the identification of every such system in the Galaxy is central to our understanding of these rare evolutionary pathways in massive stellar evolution and our interpretation of the gravitational wave universe. However, the faint X-ray luminosity of wind-accreting SyXBs, together with their locations in obscured regions of the Galactic plane render identification and detailed characterization of their optical/infrared counterparts challenging. The advent of wide-area, sensitive hard X-ray surveys, together with sensitive near-infrared (NIR) spectrographs on moderate aperture telescopes to perform characterization of the bright infrared counterparts of SyXBs is beginning to open up a new era in population studies of these unique systems. Here, we present the spectroscopic identification of a new Galactic RSG X-ray binary SWIFT J0850.8-4219, confirmed as part of an ongoing program for systematic infrared spectroscopy of unidentified Galactic plane X-ray sources.

★ E-mail: kde1@mit.edu

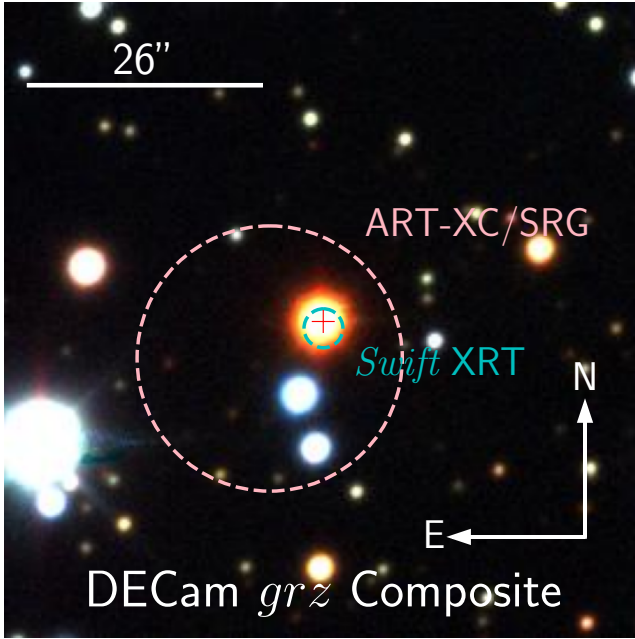


Figure 1. Optical color composite (*grz* bands) image of the localization region of SWIFT J0850.8-4219 from the DECcam Galactic Plane Survey. The image shows the 90% localization region for the X-ray source from the ART-XC catalog and follow-up with Swift XRT. The image is centered on the proposed NIR counterpart 2MASS 0850, shown with the red cross-hair.

2 OBSERVATIONS

2.1 Hard X-ray identification and localization

The hard X-ray source SWIFT J0850.8-4219 was reported in the 105-month all-sky *Swift* Burst Alert Telescope (BAT) catalog (Oh et al. 2018). It was also detected in the soft X-ray band, in two pointed observations with the *Swift* X-Ray Telescope (XRT; Burrows et al. 2005) done on 2011 December 22 and 24. An X-ray source at a very similar location was also detected with signal-to-noise ratio of 5.7 in the first data release (Pavlin et al. 2021) of the *Spektrum-Roentgen-Gamma* (SRG) Astronomical Roentgen Telescope – X-ray Concentrator (ART-XC) all-sky survey. The ART-XC detection (catalogued as SRGA J085040.6–421156) was based on data collected between 2019 December and 2020 December. The nominal positional uncertainty of the ART-XC source is $\lesssim 15''$, which makes it perfectly consistent with the *Swift*/XRT position.

We re-processed the two public archival *Swift*/XRT observations of the field with the online XRT products tool (Evans et al. 2009) to derive an enhanced position using stars in the *Swift* UltraViolet and Optical Telescope (UVOT; Goad et al. 2007) field of view. The best-fit position (J2000 coordinates) is $\alpha = 08^h 50^m 40^s.08$, $\delta = -42^\circ 11' 52''.3$, with an uncertainty of $2''.2$. The accurate XRT localization enables the identification of a possible bright NIR counterpart in the 2MASS catalog (2MASS 08504008–4211514; hereafter 2MASS 0850), located $\approx 0''.9$ from the best-fit XRT position. In Figure 1, we show an optical color composite image of the localization region using archival images from the DECcam Galactic plane survey (Schlafly et al. 2018).

The proposed NIR counterpart is reported in the 2MASS catalog (Skrutskie et al. 2006) with NIR magnitudes $J = 9.53 \pm 0.02$ mag, $H = 8.27 \pm 0.03$ mag and $K_s = 7.77 \pm 0.02$ mag.

Following Kaplan et al. (2007), we use the 2MASS catalog to estimate a spatial density of $\approx 2 \times 10^{-6}$ arcsec $^{-2}$ for sources brighter than $K_s = 8.0$ in a 10 arcmin radius around the source. This suggests a random probability of $\approx 5 \times 10^{-6}$ for the X-ray source to be spatially coincident within $\approx 0''.9$ of the bright IR source. We therefore conclude that 2MASS 0850 is the likely IR counterpart of SWIFT J0850.8-4219.

2.2 SOAR/TSpec Observations

On UT 2022-05-12, we obtained a NIR spectrum of 2MASS 0850 using the TripleSpec spectrograph (Schlawin et al. 2014) on the 4.1 m Southern Astrophysical Research Telescope (SOAR; program 2022A-881609, PI: De). The data were acquired as a series of dithered exposures with ABBA dither pattern, amounting to a total exposure time of 240 s. We also obtained exposures of the A0V telluric standard HIP 45079. The data were reduced using the *spectool* package (Cushing et al. 2004) followed by telluric correction and flux calibration using the *xtellcor* package (Vacca et al. 2003). Figure 2 shows the $1.0 - 2.5 \mu\text{m}$ spectrum of 2MASS 0850. The spectrum exhibits a red continuum peaking in *H*-band together with deep absorption features of the CO first overtone starting at $\approx 2.29 \mu\text{m}$, characteristic of late K-M giants and supergiants. In *Y*-band, we identify a very strong emission line of the He I 10830 line, with an equivalent width of $-6.2 \pm 0.1 \text{ \AA}$. The strong emission line is indicative of a hot source (i.e. a compact object) ionizing the wind of the star since isolated late-type giants exhibit much weaker He I lines ($|EW| \ll 1 \text{ \AA}$; Dupree et al. 2009), confirming the association of the infrared source with the hard X-ray counterpart.

3 ANALYSIS

3.1 Spectroscopic diagnostics

We use equivalent widths (EWs) measured from the NIR spectrum of 2MASS 0850 to constrain the spectral type and luminosity class of the donor star in SWIFT J0850.8-4219. We use the wavelength regions defined by Messineo et al. (2021) to measure the EWs of the spectral features. The equivalent width of the $^{12}\text{CO}(2,0)$ bandhead is $35.8 \pm 0.8 \text{ \AA}$. We clearly detect absorption features of Na I (at $2.207 \mu\text{m}$) and Ca I (at $2.263 \mu\text{m}$) in *K*-band, with equivalent widths of $2.2 \pm 0.3 \text{ \AA}$ and $3.1 \pm 0.3 \text{ \AA}$ respectively. Together we measure the $\log[EW(\text{CO})/(EW(\text{Na})+EW(\text{Ca}))]$ to be ≈ 0.83 , squarely pointing to the classification of this source as a late-type giant or supergiant, as late-type dwarfs occupy a different parameter space in this ratio (Ramirez et al. 1997).

If we assume the source to be a giant as seen in most other SyXBs, the relationship between the $^{12}\text{CO}(2,0)$ EW and effective temperature in Ramirez et al. 1997 would suggest a spectral type of $\approx \text{M5-M6}$, corresponding to an effective temperature of $\approx 3500 \text{ K}$. In Figure 2, we show a comparison of the full and *Y + J*-band spectrum of a M6-III giant in the IRTF spectral library (Rayner et al. 2009) to 2MASS 0850. As shown, there are striking differences in features that are known to distinguish giants and supergiants (Messineo et al. 2021) – i) the presence of strong CN features in 2MASS 0850, but weak in the M6-III template, and ii) the absence of a strong TiO bandhead at $\approx 1.1 \mu\text{m}$ in 2MASS 0850, clearly present in the M6-III template and ubiquitously seen in giants of this spectral type.

As supergiants occupy a different relationship between the CO absorption strength and spectral type (owing to their lower surface gravity, which strengthens the CO band for a given temperature),

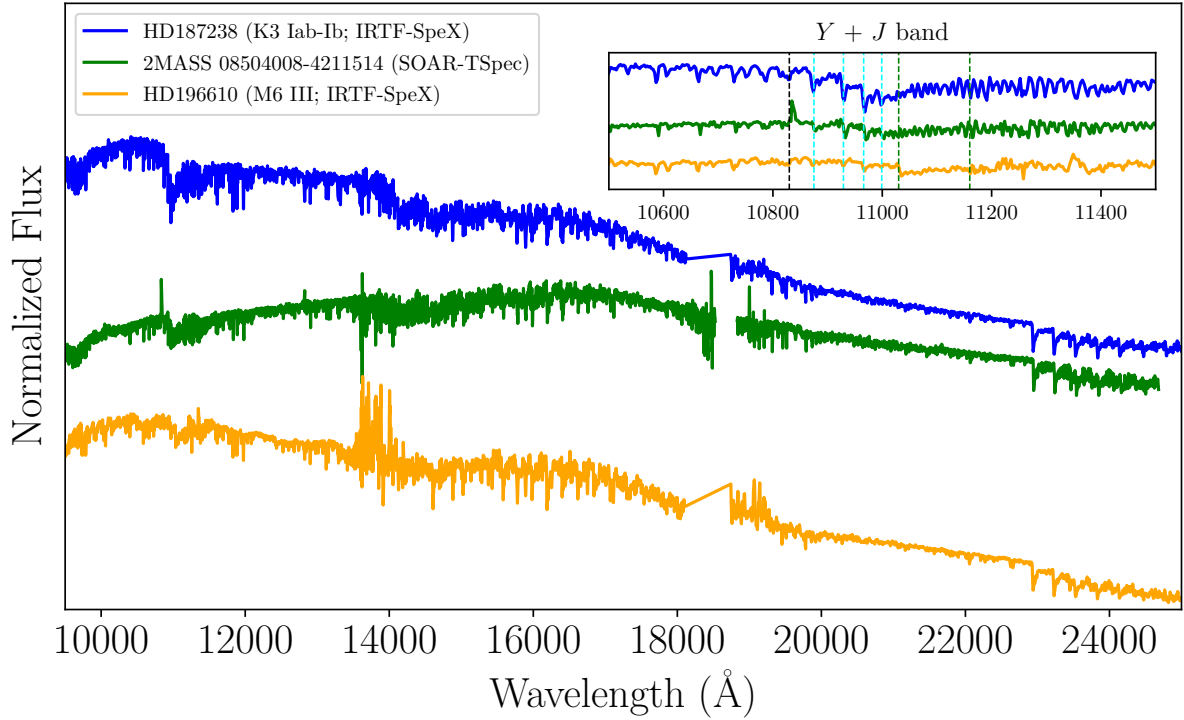


Figure 2. NIR spectrum of 2MASS 0850, the proposed infrared counterpart of SWIFT J0850.8-4219, compared to late-type stars in the IRTF spectral library (Rayner et al. 2009). We show comparisons against the two possible classifications of the source – a M6-III giant or a K3 supergiant. The inset shows the spectra zoomed into the region covering Y and J band, highlighting the He I 10830 Å feature (black dotted line), strong CN lines (cyan dotted line) seen in supergiants and the TiO bandhead (green dotted line) seen only in late-type giants (but not in 2MASS 0850). The continuum shape has not been corrected for foreground extinction, and hence the redder continuum of 2MASS 0850 reflects the larger foreground extinction to the source.

we use the calibration of Blum et al. (2003) to estimate the corresponding effective temperature and spectral type. We measure the CO index, as defined in Blum et al. (2003), to be 19.27 ± 0.05 in 2MASS 0850. The corresponding effective temperature would be 3820 ± 10 K. Messineo et al. (2021) show that effective temperatures derived from infrared diagnostics typically have a systematic scatter of ≈ 100 K from those derived from optical spectroscopic features (the TiO bandhead; Dorda et al. 2016b,a), and we therefore adopt the temperature to be 3820 ± 100 K. The corresponding spectral type is $\approx K3-K5$ based on the temperature scale of Levesque et al. (2005).

In Figure 2, we also show a comparison of the spectrum of a K3 supergiant to 2MASS 0850 showing better consistency in the spectral features. To quantify these qualitative differences, we turn to the infrared spectral indices presented by Messineo et al. (2021). They show that giants and supergiants can be differentiated based on their Mg I 1.71 μ m and CO 2.29 μ m equivalent widths. We measure the Mg I 1.71 μ m EW to be 2.3 ± 0.2 Å, placing this source in the region occupied by supergiants (Figure 3). We further measure the J8, J9 and J10 indices defined in Messineo et al. (2021), which have been used to detect CN absorption that is ubiquitously seen in RSGs, but weak or absent in giants. We find that the source again lies in the region squarely occupied only by supergiants in the phase space of J8+J9+J10 (measured to be $\approx 3.8 \pm 0.2$ Å) against CO EW (Figure 3). Together, we classify 2MASS 0850 to be a RSG with a spectral type of $\approx K3-K5$.

3.2 Distance, extinction and system parameters

The integrated Galactic extinction along the line of sight to 2MASS 0850 is $A_V \approx 7.0$ mag (Schlafly & Finkbeiner 2011), and therefore sufficiently large to affect the brightness and color of the source. In order to estimate the distance and absolute luminosity of 2MASS 0850, we take the typical NIR colors of K3 RSGs of $J - K \approx 0.7$ mag (Messineo & Brown 2019) together with the observed 2MASS colors to obtain a foreground extinction of $A_V \approx 5.3$ mag. The reported parallax of the source in Gaia DR3 (Gaia Collaboration et al. 2023) is $\approx 0.08 \pm 0.01$ mas, corresponding to a distance range of $\approx 11 - 14$ kpc. Correcting for foreground extinction, we estimate the absolute magnitude of the source to be in the range $M_K \approx -8.0$ to ≈ -8.5 mag, strikingly consistent with the average absolute magnitude of K3 RSGs ($M_K \approx -8.2$ mag; Messineo & Brown 2019). Adopting 12 kpc as the distance (corresponding to $M_K = -8.2$ mag), the corresponding average bolometric luminosity and stellar radius (assuming a blackbody stellar surface) are $\approx 1.7 \times 10^4 L_\odot$ ($\log L_{\text{bol}}/L_\odot \approx 4.23$) and $\approx 300 R_\odot$ respectively.

3.3 X-ray properties

We stacked the data from the two *Swift*/XRT observations and built a spectrum with the online XRT products tool (Evans et al. 2009). The combined exposure time is 4.8 ks. We fitted the 0.3–10 keV spectrum with XSPEC, version 12.12.0 (Arnaud 1996). Because of the limited number of counts (only ≈ 130), we could only use a simple power-law model with photoelectric absorption (*tbabs* \times *pow* in XSPEC). We grouped the spectrum to a minimum of 1 count per bin and used

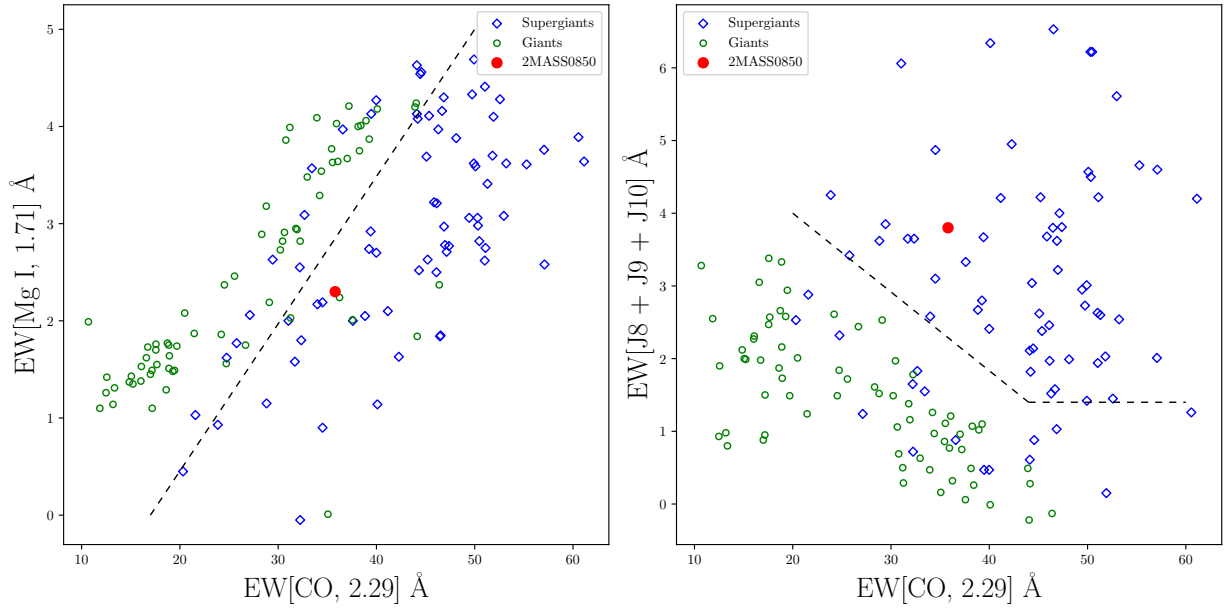


Figure 3. Comparison of the equivalent widths of 2MASS 0850 to giants and supergiants presented [Messineo et al. \(2021\)](#). The left plot shows the position of the source in the diagram of Mg I against CO, with the black dashed line separating the regions occupied by giants and supergiants (supergiants occupy the region to the right of the line) as proposed by [Messineo et al. \(2021\)](#). The right plot shows the same in the combination of the J8 + J9 + J10 indices against CO, with supergiants occupying the region above the black dashed line.

the *cstat* fit statistic ([Cash 1979](#)). We calculated the absorbed and unabsorbed flux and luminosity with the *cflux* convolution model. The best-fitting parameters are listed in Table 1, and the spectral fit with its data/model ratio is illustrated in Figure 4.

The unabsorbed 0.3–10 keV luminosity from the XRT is $L_{0.3-10} \approx (1.2 \pm 0.2) \times 10^{35} \text{ erg s}^{-1}$. This is consistent with the results reported in the ART-XC catalog ([Pavlinisky et al. 2021](#)) over the 4–12 keV band: $f_{4-12} \approx 8.8^{+3.2}_{-2.6} \times 10^{-12} \text{ erg cm}^{-2} \text{ s}^{-1}$; $L_{4-12} \approx 1.5^{+0.5}_{-0.2} \times 10^{35} \text{ erg s}^{-1}$. It suggests that the source has not varied significantly during the nine years between the *Swift*/XRT and *SRG*/ART-XC observations. In addition, a hard X-ray flux $f_{14-195} \approx 12.1^{+2.0}_{-3.0} \times 10^{-12} \text{ erg cm}^{-2} \text{ s}^{-1}$, corresponding to a luminosity $L_{14-195} \approx 2.1^{+0.3}_{-0.5} \times 10^{35} \text{ erg s}^{-1}$, was reported in the BAT catalog ([Oh et al. 2018](#)) over the 14–195 keV band. In summary, we estimate a total X-ray luminosity $L_X \approx (4 \pm 1) \times 10^{35} \text{ erg s}^{-1}$.

The high X-ray luminosity exceeds that seen in accreting white dwarf systems ($\lesssim 10^{34} \text{ erg s}^{-1}$; [Mukai 2017](#)), which rules out a Cataclysmic Variable identification. At the same time, the unusually hard photon index $\Gamma < 1$ in the 2–10 keV band (Table 1) is inconsistent with the typical range of photon indices observed in the low/hard state of stellar-mass BHs, that is $1 < \Gamma \lesssim 2$ at similar luminosities ([Remillard & McClintock 2006](#); [Plotkin et al. 2013](#); [Yang et al. 2015](#); [Liu et al. 2019](#)). The photon index is also much lower than those observed in low-mass X-ray binaries powered by weakly magnetized NSs ([Wijnands et al. 2015](#)). It is instead perfectly consistent ([Reig & Nespoli 2013](#); [Farinelli et al. 2016](#)) with the photon indices observed from accreting, strongly magnetized NSs (X-ray pulsars) in HMXBs. The spatial association with a bright 2MASS star further supports the scenario of a young, strongly magnetized NS accreting from a RSG. Thus, we conclude that SWIFT J0850.8-4219 is most likely a newly identified Galactic SyXRB with a RSG donor.

3.4 Supergiant wind and accretion rate

A further test on the SyXRB scenario is whether the wind from the relatively faint RSG 2MASS 0850 can provide enough matter to the accreting NS to explain the system’s X-ray luminosity. The mass accretion rate onto the NS can be approximated as

$$\dot{M} \approx 2.5\pi G^2 M_{\text{ns}}^2 \rho_w v_{\text{rel}}^{-3} \quad (1)$$

([Bondi & Hoyle 1944](#)), where $M_{\text{ns}} \approx 1.4M_{\odot}$ is the mass of the NS, ρ_w is the density of the RSG wind at the orbit of the NS, and $v_{\text{rel}} \approx (v_w^2 + v_K^2)^{1/2}$ is the relative velocity of stellar wind and compact object, function both of the intrinsic wind speed v_w and of the Keplerian orbital speed v_K of the NS. The wind density is related to the RSG mass loss rate \dot{M}_w as

$$\dot{M}_w = 4\pi a^2 \rho_w(a) v_w(a) \quad (2)$$

where a is the binary separation. The wind speed depends on metallicity and other properties of the RSG star, but is generally observed to be $\sim 10\text{--}30 \text{ km s}^{-1}$ ([van Loon et al. 2001](#); [Goldman et al. 2017](#)). That also implies that the dominant contribution to the relative speed comes from the orbital motion of the NS, rather than from the wind speed (the opposite as in blue supergiant systems). For simple order-of-magnitude estimates, we can assume that the mass of the NS is much lower than the mass of the RSG donor ($M \sim 10\text{--}20M_{\odot}$), and we can take the simple case of a circular orbit. Then, the Keplerian speed $v_K \approx 100 (M/15M_{\odot})^{1/2} (a/300R_{\odot})^{-1/2} \text{ km s}^{-1}$. For plausible binary separations $a \lesssim 10^3 R_{\odot}$, corresponding to orbital periods $P \lesssim 10^3 \text{ d}$, we can also approximate $v_{\text{rel}} \approx v_K$.

This provides a simple estimate for the fraction of RSG wind accreted by the NS, from the ratio of equations (1) and (2):

$$\frac{\dot{M}}{\dot{M}_w} \approx 0.03 \left(\frac{M_{\text{ns}}}{1.4M_{\odot}} \right)^2 \left(\frac{M}{15M_{\odot}} \right)^{-3/2} \left(\frac{a}{300R_{\odot}} \right)^{-1/2} \left(\frac{v_w}{20 \text{ km s}^{-1}} \right)^{-1} \quad (3)$$

Determining the RSG mass loss rate is notoriously one of the critically unsolved problems of stellar evolution. For a given observed luminosity, model estimates and empirical constraints of \dot{M}_w can vary by three orders of magnitude, from $\sim a \text{ few } 10^{-9} M_\odot \text{ yr}^{-1}$ to a few $10^{-6} M_\odot \text{ yr}^{-1}$ (van Loon et al. 2005; Ekström et al. 2012; Meynet et al. 2015; Beasor et al. 2020; Humphreys et al. 2020; Wang et al. 2021; Massey et al. 2023). For our purpose, we take a value $\dot{M}_w \sim 10^{-7} M_\odot \text{ yr}^{-1}$, in the middle of the range of published values, for a luminosity $L_{\text{bol}} \approx 10^{4.23} L_\odot$. This corresponds to an accretion rate $\dot{M} \sim 2 \times 10^{17} \text{ g s}^{-1}$ for the fiducial parameters in Equation (3), and a corresponding luminosity $L_X \sim 3 \times 10^{37} \text{ erg s}^{-1}$ (for efficient accretion onto the NS surface, $\eta \approx 0.2$). Thus, our estimate shows that the wind of a RSG donor can indeed provide sufficient mass accretion to explain the X-ray luminosity of SWIFT J0850.8-4219. Even with the lower mass loss rates ($\dot{M}_w \sim 10^{-8} M_\odot \text{ yr}^{-1}$) proposed by Beasor et al. (2020), the accretion rate is more than enough to produce the observed luminosity.

The next challenge of our scenario is to explain why the observed L_X is only $\sim 10^{35} \text{ erg s}^{-1}$ rather than $\sim 10^{37} \text{ erg s}^{-1}$. A similar issue was discussed by Hinkle et al. (2020) in relation to the relatively low luminosity of the SyXRB 4U 1954+31. In that case, the explanation suggested by Hinkle et al. (2020) was that the system had a very large binary separation, with a period of (at least) several years, so that \dot{M}/\dot{M}_w is much reduced. For our adopted mass loss rate $\dot{M}_w \sim 10^{-7} M_\odot \text{ yr}^{-1}$, and under the assumption of efficient accretion onto the NS surface, we would need a ratio $\dot{M}/\dot{M}_w \sim 4 \times 10^{-4}$ to explain the low observed luminosity.

From Equations (1–2), we can recalculate the ratio \dot{M}/\dot{M}_w for the more general case of $v_w \gtrsim v_K$, a regime valid at large binary separations. We estimate that the binary separation would have to be $a \sim 25,000 R_\odot$ to justify the low observed luminosity. This would imply an unlikely binary period $P \approx 10^{11} \text{ s} \approx 10^5 \text{ d} \approx 300 \text{ yr}$. Extreme fine tuning would be required to produce a system with such marginal binding energy. Even for a lower mass loss rate $\dot{M}_w \sim 10^{-8} M_\odot \text{ yr}^{-1}$, we would still need $a \sim 8,000 R_\odot$ and $P \approx 50 \text{ yr}$. Thus, we regard this scenario as implausible.

Instead, we suggest that a more likely explanation is that SWIFT J0850.8-4219 is in the propeller state (Illarionov & Sunyaev 1975; Ghosh & Lamb 1979; Stella et al. 1986), in which most of the accretion flow is stopped at the magnetospheric radius. The minimum accretion luminosity below which a magnetized NS is expected to switch to the propeller state is

$$L_{\text{acc,m}} \approx 1.3 \times 10^{37} B_{12}^2 P_s^{-7/3} M_{1.4}^{-2/3} R_6^5 \text{ erg s}^{-1} \quad (4)$$

(Campana et al. 2018), where B_{12} is the surface magnetic field in units of 10^{12} G , P_s is the spin period in seconds, $M_{1.4}$ is the mass of the NS in units of $1.4 M_\odot$, and R_6 is the NS radius in units of 10^6 cm . We speculate that the accretor in SWIFT J0850.8-4219 is a young NS with $B \sim a \text{ few } 10^{12} \text{ G}$ and $P_s \lesssim 1$, so that the accretion rate supplied by the RSG wind is (currently) not enough to keep it in the accretor state.

4 SUMMARY

In this paper, we present the identification, confirmation and classification of the NIR counterpart to the hard X-ray source SWIFT J0850.8-4219. Using re-analysis of archival X-ray data and new infrared spectroscopic observations, we show

- Using archival Swift XRT observations, we localize the X-ray source (with a positional uncertainty of $2.2''$) to be coincident within

Table 1. Best-fitting parameters of the *Swift*/XRT spectrum of X-1. The model is $tbabs \times powerlaw$, and was fitted with the Cash statistics. Uncertainties correspond to $\Delta C = \pm 2.706$, which is asymptotically equivalent to the 90% confidence limit in the χ^2 statistics.

Model Parameters	Values
N_H (10^{22} cm^{-2})	$3.3^{+2.7}_{-1.9}$
Γ	$0.3^{+0.7}_{-0.6}$
N_{po}^a	$1.5^{+3.5}_{-1.0}$
C-stat/dof	110.0/128 (0.86)
$f_{0.3-10}$ ($10^{-12} \text{ erg cm}^{-2} \text{ s}^{-1}$) ^b	$5.9^{+1.7}_{-1.2}$
$L_{0.3-10}$ ($10^{35} \text{ erg s}^{-1}$) ^c	$1.2^{+0.2}_{-0.2}$

^a: units of $10^{-4} \text{ photons keV}^{-1} \text{ cm}^{-2} \text{ s}^{-1}$ at 1 keV.

^b: observed flux in the 0.3–10 keV band

^c: isotropic unabsorbed luminosity in the 0.3–10 keV band, at a distance of 12 kpc.

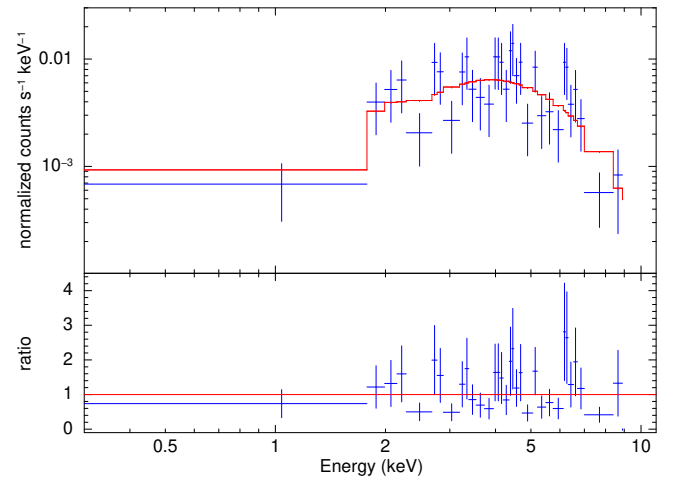


Figure 4. *Swift*/XRT spectrum from the combined datasets of 2012 December, with best-fitting power-law model and data/model ratios (see Table 1). The data have been rebinned to a signal-to-noise ratio > 1.8 for plotting purposes.

$0.9''$ of the bright NIR source 2MASS 08504008-4211514. We estimate the chance coincidence probability of the X-ray source being coincident with a NIR source at this brightness to be $\approx 5 \times 10^{-6}$ given the IR source density at this position, supporting the identification of the NIR source as the likely counterpart.

- We present a $1.0 - 2.5 \mu\text{m}$ NIR spectrum of the counterpart obtained with the SOAR telescope. The spectrum shows typical features of a late-type star together with a strong He I emission line ($\text{EW} \approx -6.2 \pm 0.1 \text{ \AA}$). The strong emission line is not seen in isolated late-type giants, and argues for the presence of a hot ionizing source near the giant, thereby confirming the identification of the counterpart.

- Using the CO bandhead at $2.29 \mu\text{m}$ to identify the spectral type of the star, we qualitatively show that the spectrum is inconsistent with a giant of the spectral type ($\approx M5-M6$) suggested by the EW of the CO bandhead, but is instead consistent with a RSG of spectral type $\approx K3-K5$ and effective temperature $3820 \pm 100 \text{ K}$. We quantitatively show that the EWs of the CO $2.29 \mu\text{m}$ bandhead, the Mg I $1.71 \mu\text{m}$ absorption feature, and in particular, the strong CN bandheads at $\approx 1.1 \mu\text{m}$ are inconsistent with those seen in late-type giants, but are instead consistent with a RSG (Messineo et al. 2021).

- Using the inferred spectral type of the RSG from the spectroscopic diagnostics, we estimate the source to be located at a distance of ≈ 12 kpc and behind a foreground dust extinction column of $A_V \approx 5.3$ mag, consistent with the Gaia DR3 parallax of the source.

- Analyzing archival X-ray observations from Swift/XRT, SRG/ART-XC and Swift/BAT, we find the X-ray luminosity of the source to be $L_X \approx (4 \pm 1) \times 10^{35} \text{ erg s}^{-1}$, which together with the hard photon index ($\Gamma < 1$), strongly argues against an accreting white dwarf (which have $L_X \lesssim 10^{34} \text{ erg s}^{-1}$; Mukai 2017) as the compact object. The measurements are instead consistent with the parameters typically seen in accreting, strongly magnetized NSs.

- We show that the wind of the RSG is expected to provide enough material to an accreting NS for reasonable ranges of orbital periods and wind velocities to power the observed X-ray luminosity. We speculate that the $\approx 100\times$ lower observed X-ray luminosity compared to the case of efficient accretion onto the NS can be explained if the accretor is in the propeller state where most of the accretion is stopped at the magnetospheric radius.

Our new identification of SWIFT J0850.8-4219 as only the second RSG X-ray binary in the Galaxy demonstrates the potential of hard X-ray instruments with high angular resolution localization capabilities to complete our census of the local stellar graveyard and our understanding of massive stellar evolution. Systematic NIR spectroscopy of counterparts identified in future and more sensitive source catalogs from ongoing surveys will provide an unprecedented view into the Galactic X-ray binary populations.

ACKNOWLEDGEMENTS

We thank E. Kara and R. Simcoe for helpful discussions on the work. We thank M. Messineo for providing the spectral indices used in their paper. K. D. was supported by NASA through the NASA Hubble Fellowship grant #HST-HF2-51477.001 awarded by the Space Telescope Science Institute, which is operated by the Association of Universities for Research in Astronomy, Inc., for NASA, under contract NAS5-26555. RS acknowledges grant number 12073029 from the National Natural Science Foundation of China (NSFC). Based on observations obtained at the Southern Astrophysical Research (SOAR) telescope, which is a joint project of the Ministério da Ciência, Tecnologia e Inovações (MCTI/LNA) do Brasil, the US National Science Foundation's NOIRLab, the University of North Carolina at Chapel Hill (UNC), and Michigan State University (MSU).

REFERENCES

Arnaud K. A., 1996, in Jacoby G. H., Barnes J., eds, *Astronomical Society of the Pacific Conference Series* Vol. 101, *Astronomical Data Analysis Software and Systems V* p. 17

Beasar E. R., Davies B., Smith N., van Loon J. T., Gehrz R. D., Figer D. F., 2020, *MNRAS*, **492**, 5994

Blum R. D., Ramírez S. V., Sellgren K., Olsen K., 2003, *ApJ*, **597**, 323

Bondi H., Hoyle F., 1944, *MNRAS*, **104**, 273

Burrows D. N., et al., 2005, *Space Sci. Rev.*, **120**, 165

Campana S., Stella L., Mereghetti S., de Martino D., 2018, *A&A*, **610**, A46

Cash W., 1979, *ApJ*, **228**, 939

Chaty S., 2018, in Bianchi M., Jansen R. T., Ruffini R., eds, *Fourteenth Marcel Grossmann Meeting - MG14*, pp 1883–1888 ([arXiv:1510.07681](https://arxiv.org/abs/1510.07681)), doi:10.1142/9789813226609_0198

Cushing M. C., Vacca W. D., Rayner J. T., 2004, *PASP*, **116**, 362

Davidson A., Malina R., Bowyer S., 1977, *ApJ*, **211**, 366

De K., et al., 2018, *Science*, **362**, 201

De K., et al., 2022, *ApJ*, **935**, 36

Dorda R., Negueruela I., González-Fernández C., Tabernero H. M., 2016a, *A&A*, **592**, A16

Dorda R., González-Fernández C., Negueruela I., 2016b, *A&A*, **595**, A105

Dupree A. K., Smith G. H., Strader J., 2009, *AJ*, **138**, 1485

Ekström S., et al., 2012, *A&A*, **537**, A146

Evans P. A., et al., 2009, *MNRAS*, **397**, 1177

Farinelli R., Ferrigno C., Bozzo E., Becker P. A., 2016, *A&A*, **591**, A29

Gaia Collaboration et al., 2023, *A&A*, **674**, A1

Ghosh P., Lamb F. K., 1979, *ApJ*, **234**, 296

Goad M. R., et al., 2007, *A&A*, **476**, 1401

Goldman S. R., et al., 2017, *MNRAS*, **465**, 403

Hinkle K. H., Fekel F. C., Joyce R. R., Wood P. R., Smith V. V., Lebzelter T., 2006, *ApJ*, **641**, 479

Hinkle K. H., Lebzelter T., Fekel F. C., Straniero O., Joyce R. R., Prato L., Karnath N., Habel N., 2020, *ApJ*, **904**, 143

Humphreys R. M., Helmelt G., Jones T. J., Gordon M. S., 2020, *AJ*, **160**, 145

Illarionov A. F., Sunyaev R. A., 1975, *A&A*, **39**, 185

Kaplan D. L., Levine A. M., Chakrabarty D., Morgan E. H., Erb D. K., Gaensler B. M., Moon D.-S., Cameron P. B., 2007, *ApJ*, **661**, 437

Kuranov A. G., Postnov K. A., Postnov K. A., 2015, *Ast. Letters*, **41**, 114

Levesque E. M., Massey P., Olsen K. A. G., Plez B., Josselin E., Maeder A., Meynet G., 2005, *ApJ*, **628**, 973

Liu Q. Z., van Paradijs J., van den Heuvel E. P. J., 2007, *A&A*, **469**, 807

Liu H., Dong A., Weng S., Wu Q., 2019, *MNRAS*, **487**, 5335

Massey P., Neugent K. F., Ekström S., Georgy C., Meynet G., 2023, *ApJ*, **942**, 69

Messineo M., Brown A. G. A., 2019, *AJ*, **158**, 20

Messineo M., Figer D. F., Kudritzki R.-P., Zhu Q., Menten K. M., Ivanov V. D., Chen C. H. R., 2021, *AJ*, **162**, 187

Meynet G., et al., 2015, *A&A*, **575**, A60

Mukai K., 2017, *PASP*, **129**, 062001

Oh K., et al., 2018, *ApJS*, **235**, 4

Pavlinsky M., et al., 2021, *A&A*, **650**, A42

Plotkin R. M., Gallo E., Jonker P. G., 2013, *ApJ*, **773**, 59

Ramirez S. V., Depoy D. L., Frogel J. A., Sellgren K., Blum R. D., 1997, *AJ*, **113**, 1411

Rayner J. T., Cushing M. C., Vacca W. D., 2009, *ApJS*, **185**, 289

Reig P., Nespoli E., 2013, *A&A*, **551**, A1

Remillard R. A., McClintock J. E., 2006, *ARA&A*, **44**, 49

Schlaflly E. F., Finkbeiner D. P., 2011, *ApJ*, **737**, 103

Schlaflly E. F., et al., 2018, *ApJS*, **234**, 39

Schlawin E., et al., 2014, in Ramsay S. K., McLean I. S., Takami H., eds, *Society of Photo-Optical Instrumentation Engineers (SPIE) Conference Series* Vol. 9147, *Ground-based and Airborne Instrumentation for Astronomy V* p. 91472H, doi:10.1117/12.2055233

Skrutskie M. F., et al., 2006, *AJ*, **131**, 1163

Stella L., White N. E., Rosner R., 1986, *ApJ*, **308**, 669

Tauris T. M., van den Heuvel E. P. J., 2006, in , Vol. 39, *Compact stellar X-ray sources*. pp 623–665, doi:10.48550/arXiv.astro-ph/0303456

Tauris T. M., Langer N., Podsiadlowski P., 2015, *MNRAS*, **451**, 2123

Tauris T. M., et al., 2017, *ApJ*, **846**, 170

Vacca W. D., Cushing M. C., Rayner J. T., 2003, *PASP*, **115**, 389

Wang T., Jiang B., Ren Y., Yang M., Li J., 2021, *ApJ*, **912**, 112

Wijnands R., Degenaar N., Armas Padilla M., Altamirano D., Cavecchi Y., Linares M., Bahramian A., Heinke C. O., 2015, *MNRAS*, **454**, 1371

Yang Q.-X., Xie F.-G., Yuan F., Zdziarski A. A., Gierliński M., Ho L. C., Yu Z., 2015, *MNRAS*, **447**, 1692

Yungelson L. R., Kuranov A. G., Postnov K. A., 2019, *MNRAS*, **485**, 851

van Loon J. T., Zijlstra A. A., Bujarrabal V., Nyman L. Å., 2001, *A&A*, **368**, 950

van Loon J. T., Cioni M. R. L., Zijlstra A. A., Loup C., 2005, *A&A*, **438**, 273

This paper has been typeset from a \LaTeX file prepared by the author.